



THE PREPARATION OF Fe-TRANSITION-METAL OXIDE HOST SILICATE AS A POSITIVE ELECTRODE CANDIDATE FOR LI-ION SECONDARY BATTERIES

V.Meenakshi^a, R.Dhanalakshmi^{a,b}, R.Subadevi^a, M.Sivakumar^{a,*}

^a#120, Energy Materials Lab, Department of Physics, Alagappa University, Karaikudi-630003, Tamil Nadu.

^bDepartment of Physics, Thiagarajar College, #139-140, Kamarajar Salai, Madurai - 625009, Tamil Nadu, India.

ABSTRACT: *Lithium ironorthosilicate is one of the most promising positive electrode materials for next generation lithium-ion batteries. Among the current cathodes, $\text{Li}_2\text{FeSiO}_4$ has great attention due to good thermal stability, non-toxicity and environmental benignity. Iron orthosilicate offers good structural stability lithium intercalations in Li-ion batteries. Iron and silicon are the most abundant and lowest cost elements^[1]. It provides a nominal capacity of 332mAh/g by exchanging lithium ions during cycling^[2]. In this work, an attempt has been made to synthesize lithium ironorthosilicate via sol-gel method using TEOS (Tetraethylorthosilicate) as a silicate source. The structural property was studied by X-ray diffraction (XRD), Scanning Electron Microscope (SEM), Raman and Fourier Transform Infrared Spectroscopy (FTIR) techniques. The XRD analysis shows the prepared sample has an orthorhombic structure with the space group of Pmn_21 . FTIR analysis progresses the vibration of SiO_4 and LiO_4 tetrahedra (525 and 422 cm^{-1}). The Raman shift was identified in the range of $400\sim 700\text{ cm}^{-1}$ belongs to Fe-O vibrations.*

Key words: *Lithium ironorthosilicate, TEOS, XRD, FTIR, RAMAN, and SEM*

INTRODUCTION

Up to date, LIB plays a vital role in hybrid electric vehicles and portable electronics^[3]. An energetic candidate of positive electrode determines energy density, safety and life cycle of LIBs. Therefore, the development of cathode is still being a demand like eco-friendly, low cost and especially high-energy density and high safety^[4]. Now a days, following typical cathode structures are available based on inorganic compounds, which is layered, spinel and poly-anion structure^[5]. According to the bonding nature of transition metals with oxygen, these bonding has been classified into the full octahedron such as layered LiMO_2 ($\text{M}=\text{Ni}, \text{Co}$ and Mn)^[6], octahedron/tetrahedron hybrid such as spinel LiMn_2O_4 and full tetrahedron structures^[7]. The full tetrahedron structure (Li_2MSiO_4 , $\text{M}=\text{Fe}, \text{Co}$ and Mn) provides high theoretical capacity (332mAh/g) due to more lithium atom embedded into the structure^[8]. More recently, full tetrahedron orthosilicate ($\text{Li}_2\text{FeSiO}_4$) was proposed as a promising cathode for LIBs. The $\text{Li}_2\text{FeSiO}_4$ has much higher theoretical capacity than that of LiFePO_4 and high thermal stability appropriate to strong Si-O bonding.^[1,9,10] $\text{Li}_2\text{FeSiO}_4$ suffers from poor ionic mobility, low electronic conductivity and poor rate capability owing to full tetrahedron nature^[8]. Various techniques are available to overcome these drawbacks such as conductive material coating, metallic ion doping in Si sites and particle size reduction. Among these techniques, particle size reduction has been remarkable technique to enhance the peak properties of LIB cathode^[11-13]. Still date, various successful methods are available for the synthesis of lithium ironorthosilicate such as solid state, hydrothermal, sol-gel methods. Above methods, sol-gel method is effective method for crystalline material preparation^[14-15]. In this work, $\text{Li}_2\text{FeSiO}_4$ was synthesized via sol-gel method using TEOS as a silicate source. The structural property of prepared sample was investigated using XRD, FT-IR, RAMAN and SEM analysis. In focus, FT-IR and Raman analysis explores the status for the tetrahedral bonding of prepared sample.

EXPERIMENTAL:

The lithium ironorthosilicate prepared via sol-gel method using acetic acid as a catalyst. Lithium acetate dehydrates, iron oxalate dehydrates and TEOS (tetraethylorthosilicate) were taken in 4:1:1 ratio. Considerable amount of $\text{CH}_3\text{COOLi} \cdot 2\text{H}_2\text{O}$ and $\text{FeC}_2\text{O}_4 \cdot 2\text{H}_2\text{O}$ was dissolved in 20ml of ethanol. TEOS and 1.5 ml acetic acid were stirred with de-ionized water. After minutes, TEOS precursor was slowly added to ethanol mixer and followed continuous vigorous stirring. TEOS will react to form silicate source. The solution was evaporated at 80°C with continuous stirring to form the transparent gel. The obtained gel was dried at 150°C for 12 h. The dried powder was carried out and milled by ball milling process, and calcined at 800°C for 10 h under Ar atmosphere and to obtain final composite. This sol-gel-sol growth developed a tetrahedral network due to the formation of an oxide network through polycondensation reactions of a molecular precursor and to the proper calcined process.

Crystal structure of the prepared composite was analyzed by powder X-ray diffraction (PANalytical XPERT-PRO with Cu K α radiation), analysis in the range of 2 θ =10-80°. The functional group vibrations were identified by FT-IR spectroscopy (Thermo Nicolet 380 Instrument Corporation using KBr pellets) and Raman spectroscopy (SEKI, Japan). The surface morphology was studied by SEM analysis (FEG Quanta 250).

RESULT AND DISCUSSION

XRD ANALYSIS:

XRD analysis used to identify the phases of crystalline material and to calculate the unit cell dimension. XRD pattern of prepared composite is shown in Fig (i) the final composite has an orthorhombic structure with the space group of Pmn₂₁ and there corresponding hkl values are marked. The average crystallite size is 26 nm calculated from the Scherrer equation. The unit cell volume of the as prepared sample is 167.90 Å³. Some crystallite impurity peaks were detected like Li₂SiO₃ and Fe₂O₃. Dislocation density was described as the length of dislocation lines per unit volume for impure phase crystal structure^[16]. The dislocation density calculated by,

$$\delta = \frac{1}{d^2}$$

The dislocation density of the sample can be calculated as $\delta=0.18$. A small dislocation density is identified and it describes the crystallization nature and defects of prepared sample^[17].

FTIR ANALYSIS

The functional group vibration of the prepared sample was identified by FT-IR analysis. Fig (ii) shows the vibrational modes of prepared crystalline composite. From the table (i) SiO₄ and LiO₄ tetrahedrons were identified in prepared sample^[18]. The bands around 735 and 1062 cm⁻¹ indicate asymmetric vibration of Si-O-Si and stretching vibration of O=Si-O in Li₂SiO₃. The peaks at 1505 and 1443 cm⁻¹ assign the C-O vibrations in Li₂CO₃ owing to exposure in air.

RAMAN ANALYSIS

Raman spectroscopy analysis used to aggregate vibrational, rotational and other low frequency modes of prepared sample. Raman spectra of prepared composite was shown in Fig (iii) the Raman shifts of lithium iron orthosilicate peaks are appeared at 167, 269, 473 and 692 cm⁻¹ respectively detailed from the table (ii)^[19].

SEM ANALYSIS

The surface morphology of the sample with various magnifications was shown in Fig. (iv). From the images, it is observed that there is no homogeneous nature along with particles are agglomerated bit throughout the surface cause to surface owing to the air and the dislocation density of crystal.

CONCLUSION

In this work, lithium iron orthosilicate was synthesized by sol-gel method. The powder XRD pattern of prepared sample exhibited orthorhombic structure with Pmn₂₁ space group. The calculated dislocation density 0.18 indicates the presence of impurity phases of crystal. LiO₄ and SiO₄ tetrahedrons were identified by spectroscopy analysis excluding FeO₄ tetrahedral site due to the formation of Fe₂O₃. Subsequently the prepared cathode material provides quasi tetrahedral structure, which also benefits the enhancement of the ionic mobility, electronic conductivity and rate capability respectively. The strategy of developing a quasi tetrahedral structure has some advantages for LIBs.

REFERENCES

- [1] A. Mancini, V. R. Page and L. Malavasi. J. Mater. Chem. P, 2, 17867 (2014)
- [2] X. B. Wu, X. H. Wu, J. H. Guo, S. D. Li, R. Liu, M. J. McDonald and Y. Yang, Green Energy and Technology, PP, 93-134, (2015)
- [3] S. Esaki, M. Nishijima and T. Yao, ECS Electrochemistry Letters, Vol. 2, 10, pp. A93-A97, (2013)
- [4] S. Ranault, R. Steven, B. Daniel and E. Kristina, Chemsuschem, Vol. 7, no. 10, pp. 2859-2867, (2014)
- [5] A. K. Padhi, K. S. Nanjundaswamy, J. B. Goodenough, J. Electrochem. Soc. 144, 118-1194 (1997)
- [6] K. Kang, Y. S. Meng, J. Breger, C. P. Grey, G. Ceder, Science 311, 977-980 (2006)
- [7] D. H. Jang, Y. J. Shin, S. M. Oh, J. Electrochem. Soc. 143, 2204-2211, (1996)
- [8] S. I. Nishimura, S. HAYASE, R. Kanno, M. Yashima, N. Nakayama, A. Yamada, J. Am. Chem. Soc. 130, 13212-13213, (2008)
- [9] H. Y. Go, Z. Hu, J. G. Yang, J. Chem. Energy Technol., 2, 355-361 (2014).
- [10] H. Lee, S. D. Park, J. Moon, K. Cho, M. Cho, S. Y. Kim, Chem. Mater., 26, 3895-3899, (2014)
- [11] D. Rangappa, K. D. Murukanahally, T. Tomai, A. Cenemoto, I. Honma, Nano. Lett. 12, 1146-1151. (2012)
- [12] J. Yang, L. Hu, J. Zhang, D. He, L. Tian, S. Mu, F. Pan, J. Mater. Chem. A3, 9601-9608. (2015)

- [13] J. Yang, X. Kang, D. He, A. Zhang, M.pan, S.Mu, J. Mater. Chem . A3 , 16567 – 16573, (2015)
- [14] C.Deng, Y.H.Suo, S.Zhang, H.M.Lin, Y.Gao, B.Wu, L.Ma, Y.Shang, G.Dong, Int. J. Electrochem . Sci ., 7, 4559-4566, (2012)
- [15] A.Nyten, A. Abouimrane, M. Armand, T. Gustafsson, J. O. Thomas, J. ECC, 7, 156-160, (2005).
- [16] J. A. J aen, M. Jmenez, E. Elore, A.M unoz, J. A. Tabares, G.A. Peroz, A. Lcazar, Hyperfine Interact, 232, 127-140, (2015)
- [17] S. F. Varol, G. Babur, G. Cankaya and U. Kolemen, RSC Adv, 4, 56645, (2014)
- [18] R.Fu, Y.L I, H. Yang, Y.Zhang, X. Cheng, J. ECS, 160(5), A3048-A3053,(2013)
- [19] S. Shivani, M. Sagar, J. Elec . Chem . Acta, 123, 378-386, (2014)

FIGURE CAPTIONS

Fig (i) XRD analysis for prepared sample

Fig (ii) FT-IR analysis for prepared sample

Fig (iii) Raman analysis for prepared sample

Fig (iv) SEM analysis of prepared sample with various magnifications (40 K, 60 K and 160 k)

TABLE CAPTIONS

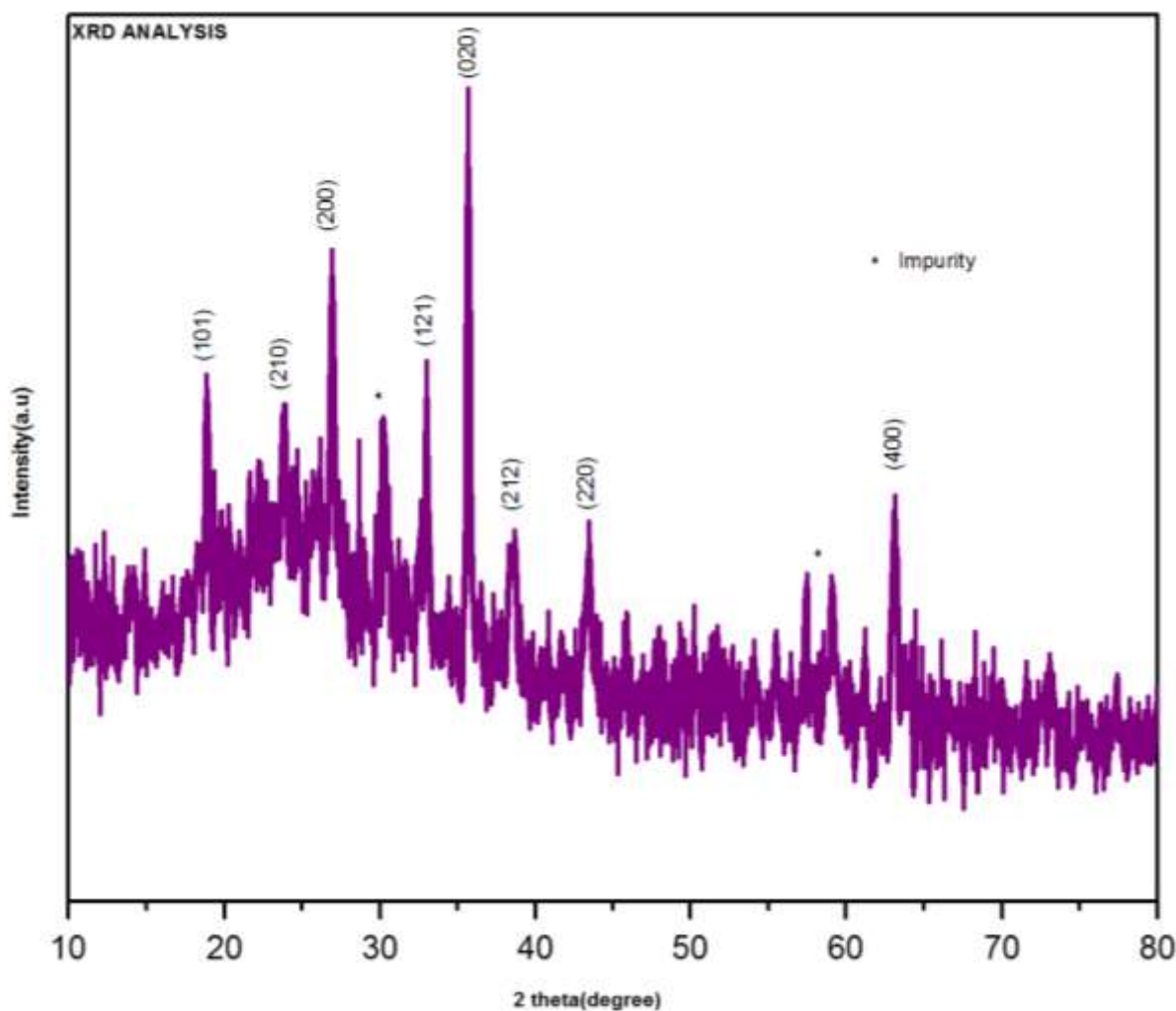
Table (i) Table for vibrational modes of prepared sample

Table (ii) Table for Raman shifts of prepared sample

Name of the author: V.Meenakshi^a, R.Dhanalakshmi^{a,b}, R.Subadevi^a, M.Sivakumar^{a,*}

Title of the manuscript: THE PREPARATION OF Fe-TRANSITION-METAL OXIDE HOST SILICATE AS A POSITIVE ELECTRODE CANDIDATE FOR LI-ION SECONDARY BATTERIES

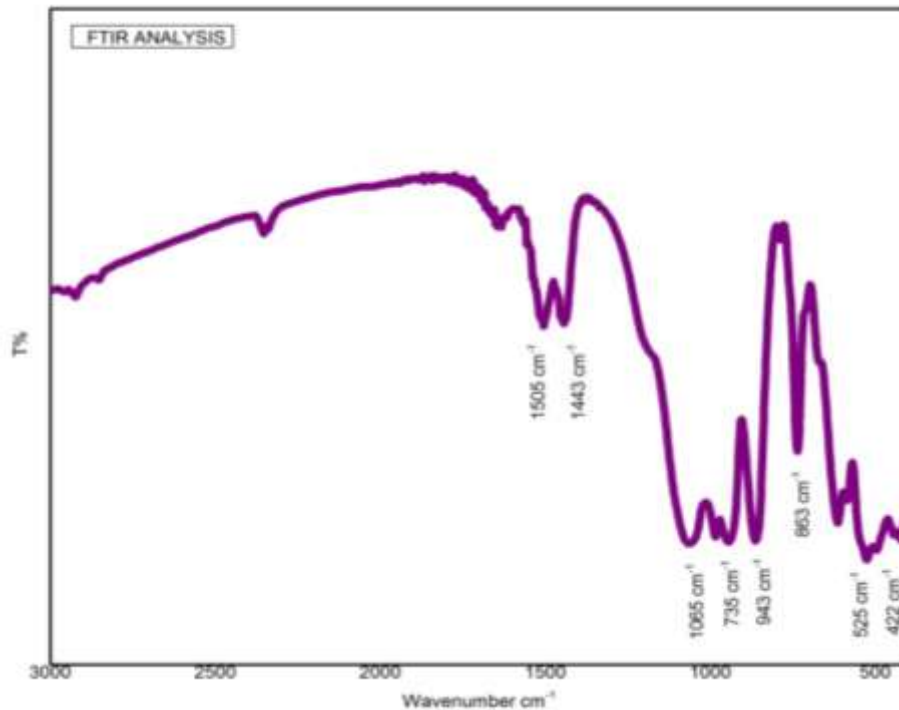
Figure (i)



Name of the author: V.Meenakshi^a, R.Dhanalakshmi^{a,b}, R.Subadevi^a, M.Sivakumar^{a,*}

Title of the manuscript: THE PREPARATION OF Fe-TRANSITION-METAL OXIDE HOST SILICATE AS A POSITIVE ELECTRODE CANDIDATE FOR LI-ION SECONDARY BATTERIES

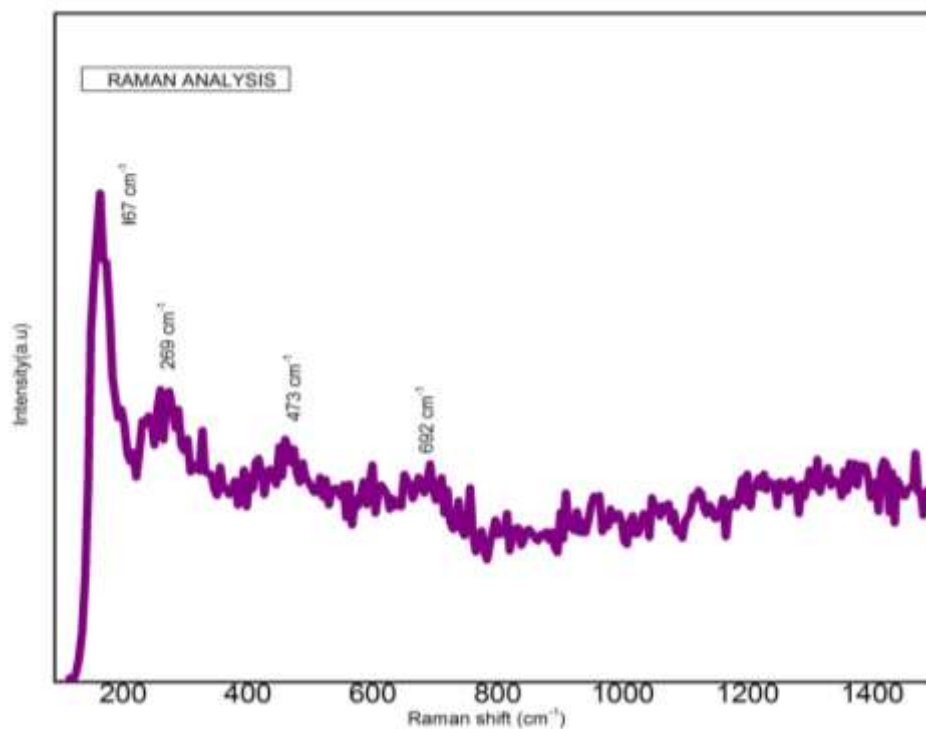
Figure (ii)



Name of the author: V.Meenakshi^a, R.Dhanalakshmi^{a,b}, R.Subadevi^a, M.Sivakumar^{a,*}

Title of the manuscript: THE PREPARATION OF Fe-TRANSITION-METAL OXIDE HOST SILICATE AS A POSITIVE ELECTRODE CANDIDATE FOR LI-ION SECONDARY BATTERIES

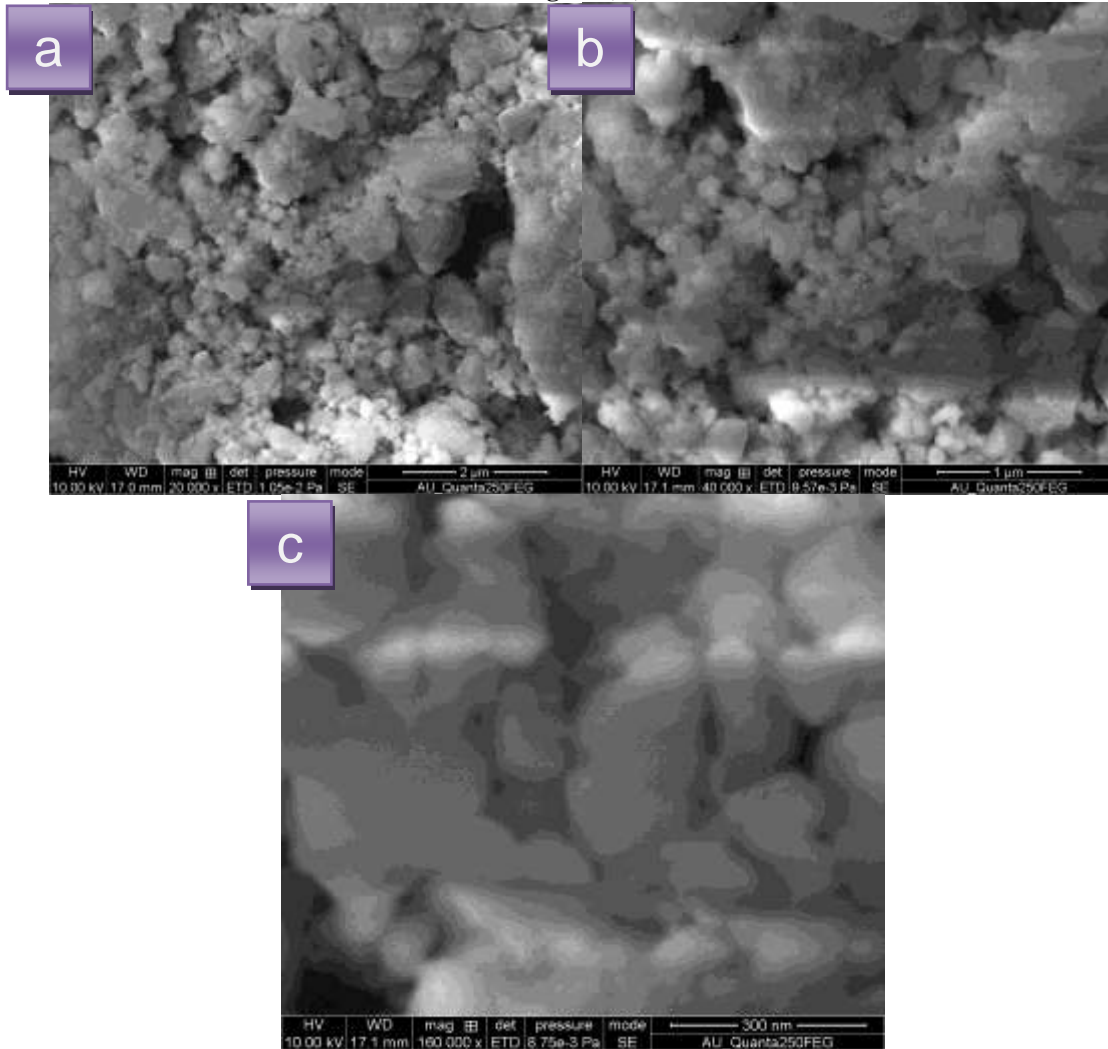
Figure (iii)



Name of the author: V.Meenakshi^a, R.Dhanalakshmi^{a,b}, R.Subadevi^a, M.Sivakumar^{a,*}

Title of the manuscript: THE PREPARATION OF Fe-TRANSITION-METAL OXIDE HOST SILICATE AS A POSITIVE ELECTRODE CANDIDATE FOR LI-ION SECONDARY BATTERIES

Figure (iv)



Name of the author: V.Meenakshi^a, R.Dhanalakshmi^{a,b}, R.Subadevi^a, M.Sivakumar^{a,*}

Title of the manuscript: THE PREPARATION OF Fe-TRANSITION-METAL OXIDE HOST SILICATE AS A POSITIVE ELECTRODE CANDIDATE FOR LI-ION SECONDARY BATTERIES

Table (i)

Wave number (cm ⁻¹)	Vibrational Modes	Presented structure
422	Bending mode of Si-O	SiO ₄
525	Bending mode of Li-O	LiO ₄
863	Stretching modes of Si-O	SiO ₄
943		

Name of the author: V.Meenakshi^a, R.Dhanalakshmi^{a,b}, R.Subadevi^a, M.Sivakumar^{a,*}

Title of the manuscript: THE PREPARATION OF Fe-TRANSITION-METAL OXIDE HOST SILICATE AS A POSITIVE ELECTRODE CANDIDATE FOR LI-ION SECONDARY BATTERIES

Table (ii)

Raman shift (cm ⁻¹)	Modes and bending
167	SiO ₄ translational mode
269	Fe translational mode
473	Si cation symmetric bending
692	O-Si-O asymmetric bending